Anal Bioanal Chem (2013) 405:159–176
DOI 10.1007/s00216-012-6471-z

ORIGINAL PAPER

δ^{15}N measurement of organic and inorganic substances by EA-IRMS: a speciation-dependent procedure

Natacha Gentile · Michel J. Rossi · Olivier Delémont · Rolf T. W. Siegwolf

Received: 30 August 2012 / Revised: 27 September 2012 / Accepted: 1 October 2012 / Published online: 26 October 2012

Abstract Little attention has been paid so far to the influence of the chemical nature of the substance when measuring δ^{15}N by elemental analysis (EA)–isotope ratio mass spectrometry (IRMS). Although the bulk nitrogen isotope analysis of organic material is not to be questioned, literature from different disciplines using IRMS provides hints that the quantitative conversion of nitrate into nitrogen presents difficulties. We observed abnormal series of δ^{15}N values of laboratory standards and nitrates. These unexpected results were shown to be related to the tailing of the nitrogen peak of nitrate-containing compounds. A series of experiments were set up to investigate the cause of this phenomenon, using ammonium nitrate (NH_4NO_3) and potassium nitrate (KNO_3) samples, two organic laboratory standards as well as the international secondary reference materials IAEA-N1, IAEA-N2—two ammonium sulphates [$(NH_4)_2SO_4$]—and IAEA-NO-3, a potassium nitrate. In experiment 1, we used graphite and vanadium pentoxide (V_2O_5) as additives to observe if they could enhance the decomposition (combustion) of nitrates. In experiment 2, we tested another elemental analyser configuration including an additional section of reduced copper in order to see whether or not the tailing could originate from an incomplete reduction process. Finally, we modified several parameters of the method and observed their influence on the peak shape, δ^{15}N value and nitrogen content in weight percent of nitrogen of the target substances. We found the best results using mere thermal decomposition in helium, under exclusion of any oxygen. We show that the analytical procedure used for organic samples should not be used for nitrates because of their different chemical nature. We present the best performance given one set of sample introduction parameters for the analysis of nitrates, as well as for the ammonium sulphate IAEA-N1 and IAEA-N2 reference materials. We discuss these results considering the thermochemistry of the substances and the analytical technique itself. The results emphasise the difference in chemical nature of inorganic and organic samples, which necessarily involves distinct thermochemistry when analysed by EA-IRMS. Therefore, they should not be processed using the same analytical procedure. This clearly impacts on the way international secondary reference materials should be used for the calibration of organic laboratory standards.

Keywords Nitrate · Nitrogen · Isotope ratio mass spectrometry · Ammonium · Elemental analysis–isotope ratio mass spectrometry · Inorganic

Introduction

Little attention has been paid so far to the influence of the chemical nature of the substance analysed when measuring δ^{15}N by elemental analysis (EA)–isotope ratio mass spectrometry (IRMS). Although the bulk nitrogen isotope analysis of organic material appears straightforward, literature from different disciplines using IRMS provides hints that the quantitative conversion of nitrate-containing compounds to nitrogen presents difficulties. In forensic science, Aranda et al. [1] needed to add activated charcoal to their nitrate

Electronic supplementary material The online version of this article (doi:10.1007/s00216-012-6471-z) contains supplementary material, which is available to authorized users.

N. Gentile (✉) · O. Delémont
Institut de Police Scientifique, Ecole des Sciences Criminelles,
University of Lausanne,
Batochime Building,
1015 Lausanne, Switzerland
e-mail: Natacha.Gentile@unil.ch

M. J. Rossi · R. T. W. Siegwolf
Laboratory of Atmospheric Chemistry, Paul Scherrer Institut,
5232 Villigen, Switzerland

samples and standards to support combustion by trapping evolving O_2. Benson et al. [2, 3] noticed significantly more depleted values for the first ammonium nitrate (NH_4NO_3) standard run in a sequence. Results from interlaboratory trials also showed that the analysis of nitrates led to unusually large variations [4–6]. In addition, such features have also been observed in the field of identification of sources of nitrate in water and soils. Several studies reported that the analysis of such analytes may produce scattered results. Silva et al. [7], followed by Spoelstra et al. [8], overcame inconsistent $\delta^{15}N$ values by adding 2 mg of sucrose to nitrate salt samples on the advice of Micromass Elemental. This sugar addition method was initially described by Noguchi [9] as an improvement of the micro Dumas method for nitrogen quantitative analysis of nitro and oxidation-resistant stable species. Noguchi observed that glucose had a beneficial effect on sample combustion. Yet, Borda and Hayward [10] reported scattered nitrogen content (%N) values of nitrate esters, despite the addition of glucose to their samples. Schindler and Knighton [11] also reported the incomplete recovery of nitrogen from nitrate when KNO_3 was analysed with the Dumas method. Although these earlier applications were related to the determination of nitrogen content using the micro Dumas method in its original version, they support the fact that the conversion of solid nitrates into pure N_2 may produce inconsistent results owing to an incomplete decomposition or reduction process. This may therefore affect $\delta^{15}N$ values when EA is coupled with IRMS. Numerous discussions among the community of isotope specialists have highlighted difficulties related to the isotope analysis of nitrates [12].

The present study originated from the observation of abnormal $\delta^{15}N$ values and nitrogen content of laboratory standards and nitrate-containing samples. This difference in behaviour indicated that the conversion of nitrates into N_2 was not complete and seemed to be related to N_2 peak tailing. These first observations initiated a series of experiments set up to determine the origin of this phenomenon.

In the first part, we report the abnormal behaviour of laboratory standards following the analysis of nitrates using the EA configuration usually employed in our laboratory. In the second part, a series of experiments are reported which involved the analysis of pure NH_4NO_3 and potassium nitrate (KNO_3) samples, two organic laboratory standards and the secondary reference materials IAEA-N1, IAEA-N2 and IAEA-NO-3 (see Table 1). Experiment 1 evaluated the addition of graphite and vanadium pentoxide (V_2O_5) in different proportions to nitrates as a possible solution to eliminate peak tailing [1, 12]. In experiment 2, another EA configuration involving an additional section of copper was used in order to see whether the tailing may originate from an incomplete reduction process. The results were compared with those obtained using the EA configuration routinely employed. Finally, in experiment 3, several method parameters (helium flow, sample delay, oxygen pressure and oxygen exclusion) were modified and their influence on the peak shape, $\delta^{15}N$ value and nitrogen content of the different substances was observed.

We demonstrate the good analytical performance of EA-IRMS when nitrates and the international secondary reference materials are analysed without O_2. The results are discussed considering the chemical nature of the substances and the thermodynamic conditions imposed by the analytical technique. We conclude that these inorganic substances should not be processed using the same analytical procedure as for organic material. This necessarily influences the way international reference material should be used for the calibration of organic laboratory standards.

Materials and method

Chemicals

Nitrogen (purity greater than 99.999 %), helium (purity greater than 99.9999 %) and oxygen gas (purity greater than

Table 1 Characteristics of the international reference materials, laboratory standards and nitrates used in experiments 1–3

Substance	Origin	Use as	Composition	Theoretical N content (wt%)	Known $\delta^{15}N$ value ± SD (‰ vs. air)
IAEA-N1	International Atomic Energy Agency	International reference material	Inorganic $(NH_4)_2SO_4$	21.2	0.4±0.2 [6]
IAEA-N2	International Atomic Energy Agency	International reference material	Inorganic $(NH_4)_2SO_4$	21.2	20.3±0.2 [6]
IAEA-NO-3	International Atomic Energy Agency	International reference material	Inorganic KNO_3	13.9	4.7±0.4 [6]
Standard 1	In-house	Laboratory standard	Organic $C_xH_yN_z$	2.1	0.4±0.2
Standard2	In-house	Laboratory standard	Organic $C_xH_yN_z$	2.4	1.0±0.2
Ammonium nitrate	Fluka	Sample	Inorganic NH_4NO_3	35.0	-
Potassium nitrate	Fluka	Sample	Inorganic KNO_3	13.9	-

SD standard deviation

99.995 %) were supplied by Messer (Lenzburg, Switzerland). Chromium(III) oxide (Cr_2O_3), silvered cobaltous–cobaltic oxide ($CoO–Co_2O_3$), 15-mm-diameter quartz wool discs, reduced copper wire (0.5 mm), quartz chips, quartz glass tubes (18.5 mm×450 mm) and tin capsules for solids (3.3 mm× 5 mm) were purchased from Säntis Analytical (Teufen, Switzerland). A prepacked CHNS reactor (no. 99.0733.10) was purchased from Lüdi (Flawil, Switzerland). Magnesium perchlorate (purity 98 % or greater), KNO_3 (purity greater than 99.0 %) and NH_4NO_3 (purity 99 % or greater) were obtained from Fluka (Buchs, Switzerland). NH_4NO_3 fertiliser was supplied by Landor (Birsfelden, Switzerland). Graphite powder (1–2 μm) and vanadium(V) pentoxide (purity 99.99 %) were supplied by Sigma-Aldrich Chemie (Buchs, Switzerland). IAEA-N1 [$(NH_4)_2SO_4$], IAEA-N2 [$(NH_4)_2SO_4$] and IAEA-NO-3 (KNO_3) were obtained from the International Atomic Energy Agency (Vienna).

Standards: selection and analysis

In the first part of the study, KNO_3 and NH_4NO_3 samples were measured between laboratory standards. Laboratory standards were plant-based materials routinely employed in the analytical sequences of bulk analyses conducted by the laboratory. Although they have a chemical composition different from that of the target samples (nitrates), they have well-known δ^{15}N values, intermediate precision and long-term stability. Standard 1 (Std1) originated from the mixture of plant materials. Standard 2 (Std2) was made from catalpa leaves. The standards were scheduled at the beginning and the end of each sequence (maximum 49 positions), as well as throughout the sequence. Blanks were inserted at different positions in the sequence to monitor any carryover effects. The laboratory standards, calibrated against international reference materials, have shown an overall intermediate precision in everyday use over several years of less than 0.2 ‰ for nitrogen on both IRMS apparatus. The calculated expanded uncertainty associated with δ^{15}N measurement of plant material is 0.2 ‰ (k=2).

In the second part, NH_4NO_3 and KNO_3 samples were analysed along with international secondary reference materials (IAEA-N1, IAEA-N2, IAEA-NO-3) inserted throughout the sample sequence. Samples run with a minimum of three replicates were bracketed at the beginning and at the end of the sequences with triplicates of international reference materials, in addition to replicates inserted throughout the sequence after a maximum of 12 samples. An empty tin capsule was run as a blank at the beginning and the end of the sequence to check for any carryover effects. Laboratory standards Std1 and Std2 were also run in the sequence to check the consistency, precision and accuracy of δ^{15}N values. Besides, the sequence design was modified to investigate particular effects. The number of replicates of samples and international reference materials was adapted from three up to ten successive replicates in order to observe the evolution of the m/z 29/28 ion current ratio baseline and the δ^{15}N value. By convention, the isotope value, denoted as the δ value, expresses the deviation of the isotope ratio of the sample in per mil (‰) compared with the international standard (atmospheric N_2 for nitrogen) [13]: $\delta=[(R_s-R_{ref})/R_{ref}]$, where R_s and R_{ref} are the isotope ratios of the sample and the reference, respectively. Table 1 summarises the characteristics of the substances used in the second part of this study, with their expected δ^{15}N value and standard deviation (SD).

Sample preparation

Samples and standards were weighed in 3.3 mm×5 mm tin capsules for solids. Weighed masses were adjusted to produce a peak amplitude similar to that of the reference gas (about 2,000 mV for m/z 28) and contained the equivalent of approximately 100 μg nitrogen. Typically, about 300 μg was used for IAEA-N1 and IAEA-N2 and 720 μg for IAEA-NO-3. For laboratory standards, about 3,200 μg and 3,500 μg bulk organic material was used for Std1 and Std2, respectively. For samples, about 300 μg NH_4NO_3 and 720 μg KNO_3 were used. Reference materials, laboratory standards and samples were stored in glass desiccators. Laboratory standards and samples were enclosed in sealed glass containers, whereas international reference materials were kept in their original container.

Additives to improve combustion

In experiment 1, samples were mixed with graphite or V_2O_5 in different proportions to assist their decomposition/combustion. The preliminary EA of graphite and V_2O_5 did not show any trace of nitrogen. Weighed masses of mixtures with graphite and V_2O_5 were likewise adjusted to contain the equivalent of approximately 100 μg nitrogen. Graphite and V_2O_5 were also added to reference materials (about 20 wt%) to observe any effect on δ^{15}N values.

Instrumentation and method

A Micro MC5 analytical microbalance (Sartorius, Göttingen, Germany) was used to weigh samples and standards for isotope analysis.

A NewClassic MF ML204 analytical balance (Mettler Toledo, Greifensee, Switzerland) was used to weigh the different quantities of chemicals necessary to produce the mixtures with graphite and V_2O_5. Analyses were performed with a 1110 elemental analyser (Carlo Erba, Milan, Italy) coupled with a Conflo II interface to a Delta S isotope ratio mass spectrometer (both from Finnigan MAT, Bremen, Germany). Owing to instrument availability, some of the analyses were

also performed using the same elemental analyser coupled to a DeltaPlus XP isotope ratio mass spectrometer (Finnigan MAT, Bremen, Germany). The interface parameters were 0.8-bar helium and 0.8-bar reference gas. The pressure of helium and O_2 at the regulator of the elemental analyser was 150 kPa and 50 kPa, respectively. A Zero Blank autosampler (Costech Analytical Technologies, Valencia, CA, USA) was used in order to avoid possible interferences with atmospheric N_2 and moisture. Before the measurements were started, the autosampler was evacuated for 30 min and subsequently refilled with helium. The sample was dropped from the autosampler into a combustion reactor, consisting of a heated quartz tube filled with Cr_2O_3 and silvered $CoO–Co_2O_3$, held at 1,020 °C. By means of flash combustion, also known as Dumas combustion, the sample is processed in the presence of excess oxygen. The analytical cycle, lasting 70 s, was as follows. Oxygen was injected into the combustion reactor for 60 s from the beginning of the analytical cycle. The sample was dropped 18 s after the beginning of the cycle (analytical cycle set-up: cycle lasting 70 s, oxygen injection for 60s, sample start and stop at 18 and 20 s, respectively). The gaseous products are carried in a helium flow (80 ml/min) to a reduction reactor packed with reduced copper wire, held at 650 °C. This reduction step converts nitrogen oxides into N_2 and traps the excessive oxygen. Water is captured by a magnesium perchlorate trap. The resulting gases are separated by a PoropaQ gas chromatography column (4 m, 50 °C) before entering the ion source via the Conflo II interface. The molecules are then ionised and accelerated at approximately 3,040 V. A magnetic field deflects the ions and separates the molecules according to their mass-to-charge ratio (*m*/*z*) before they reach an array of Faraday cups positioned such that ions with *m*/*z* 28, 29 and 30 are collected separately. The time for the procedure was extended to 600 s to ensure the total elution of CO for samples containing carbon. Raw data were processed with Isodat 2.0 (Thermo Fisher, Bremen, Germany).

Elemental analyser configurations

In the first part of the study, a combustion reactor, held at 1,020 °C, consisting of a quartz tube filled with Cr_2O_3 and silvered $CoO–Co_2O_3$ (combustion reactor 1 in Fig. 1) was used with a reduction reactor filled with reduced copper wire. In the second part, another elemental analyser configuration using a different combustion reactor was used in experiment 2. It consisted of a pre-packed tube for CHNS analyses, maintained at 1,020 °C, containing tungsten(VI) oxide (WO_3) on alumina (Al_2O_3) and pure electrolytic copper wire (combustion reactor 2 in Fig. 1). A reduction quartz reactor, held at 650 °C and packed with reduced copper, was combined with each combustion system, forming elemental analyser configuration systems 1 and 2 (referred to further as systems 1 and 2 for the sake of simplicity) (Fig. 1).

Variations of the method parameters

Low (60 ml/min) and high (95 ml/min) helium flows were tested. The O_2 pressure at the regulator of the elemental analyser was modified to 100 kPa and 150 kPa. The effect of suppressing the O_2 injection was also investigated. Sample

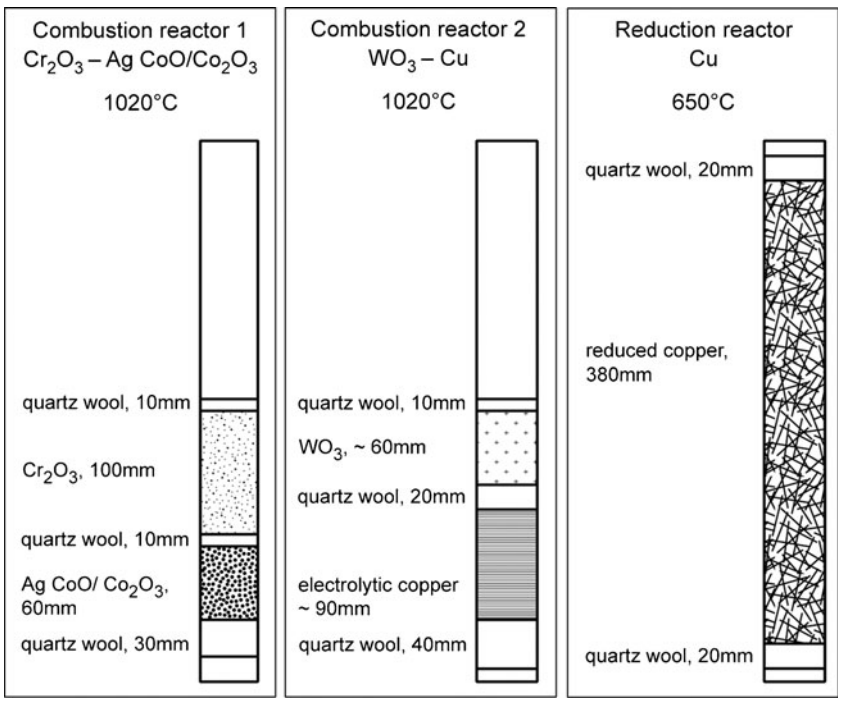

Fig. 1 Composition of the combustion and reduction reactors

delay (sample start and stop) was modified to introduce the sample at 0, 5, 10, 55 and 62 s within the analytical cycle.

Data correction (normalisation)

In the first part of the study, laboratory standards were used to correct raw data to the international scale, whereas in the second part, international secondary reference materials were used, following a two-point linear normalisation whenever possible [14]. IAEA-N2 was occasionally used alone to correct data when the peak shape, δ^{15}N value and nitrogen content of the other reference materials indicated the results were inadequate for correction. The nitrogen content (in weight per cent) was calculated on the basis of integrated peak areas of the major isotopes and determined against the theoretical nitrogen content of IAEA-N2 (21.2 wt%).

Statistical tests, quality control and uncertainty measurement

The Grubbs test was used within each sequence to determine and exclude outliers in the raw data set. Control charts were used to check the quality of the analytical response. Upper and lower warning lines were set at μ±2SD and upper and lower action lines were set at μ±3SD [15]. Differences between means were evaluated using analysis of variance [16]. The expanded uncertainty U was calculated according to the literature and using type A evaluation [17]. The expanded uncertainty was estimated at a coverage factor of 2 (k=2).

Results and discussion

Part I: unexpected behaviour of laboratory standards

Both laboratory standards Std1 and Std2 showed an intermediate precision smaller than 0.2 ‰ over a 24-month period, as illustrated by the control chart of Std1 in Fig. 2. After exclusion of the enriched δ^{15}N values corresponding to the phenomenon described in the next paragraph, the calculated intermediate precision of Std1 is 0.1 ‰ (n=217).

The unusual behaviour of Std1 (illustrated by the outlying values between measurements 127 to 222 in Fig. 2) was also observed for Std2.

Figure 3 shows the abnormal behaviour of laboratory standards, run alternatively with blanks and NH_4NO_3 samples in an analytical sequence. The δ^{15}N value of the first replicate of the laboratory standard in the sequence (in positions 7, 12, 25 and 40) following a nitrate sample was always more enriched than the other replicates and increased along the sequence (Std2 in Fig. 3a). δ^{15}N values of other replicates were not affected by this phenomenon. As the same effect was noticed for Std1 and Std2 analysed after NH_4NO_3 and KNO_3 samples, this phenomenon appears to be related to the type of substance analysed. The intensity of the phenomenon did not decrease when analysing samples containing less nitrogen [NH_4NO_3 fertiliser (27 %N) or KNO_3 (13.9 %N)] than pure NH_4NO_3 samples (35 %N). Conversely, whereas the first δ^{15}N value of a series of NH_4NO_3 replicates was more depleted than the following values, the δ^{15}N value of NH_4NO_3 samples tended to stabilise after a few samples. However, differences of up to 2 ‰ between nitrate replicates could be observed. One NH_4NO_3 measurement stands apart from the other replicates, with a δ^{15}N value of 4.1 ‰.

In addition, the variations of the δ^{15}N values of laboratory standards (Fig. 3a) seemed to be correlated with the deviations of their nitrogen contents (Fig. 3b). Whereas NH_4NO_3 samples and fertiliser exhibited a negative difference in the nitrogen content of around 2–3 % below the expected value, the first laboratory standard analysed immediately after a nitrate-containing compound displayed a slight positive deviation (Fig. 3b). A zoom-in on the y scale shows more clearly this subtle positive deviation and even reveals a slight deviation in the nitrogen content of the second or third replicate scheduled later in the time sequence (Fig. 3c).

Curiously, blanks did not allow the detection of this phenomenon. Indeed, blanks run in positions 4, 6, 10, 14 and 24 of the sequence (indicated by black arrows in Fig. 3a) did not produce nitrogen peaks. This supports the hypothesis that some nitrogen is retained in the elemental analyser and influences the δ^{15}N value of other measured

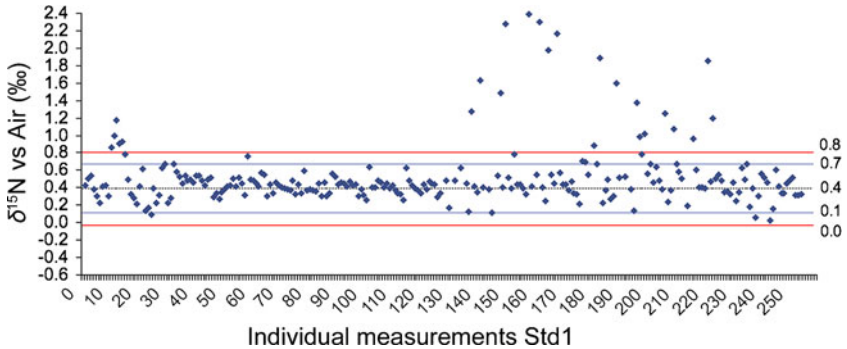

Fig. 2 Control chart of the δ^{15}N value of standard 1 (*Std1*) (N=253). The enriched δ^{15}N values (between measurements 127 and 222) correspond to the phenomenon observed and illustrated in Fig. 3. The intermediate precision calculated after exclusion of values lying outside the action limits is 0.1 ‰ (n=217)

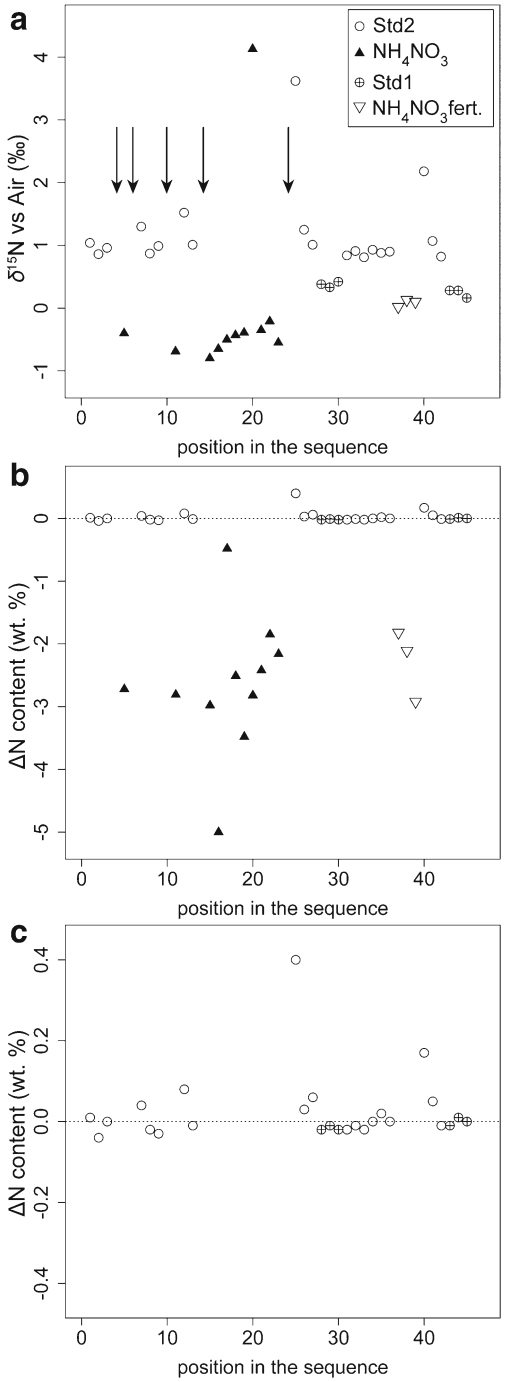

Fig. 3 **a** $\delta^{15}N$ value of NH_4NO_3 samples run alternatively in a sequence with laboratory standards Std1 and Std2, as well as blanks (their position is highlighted by *black arrows*). Note the odd value of the first replicate of a series of standards, as well as the increasing $\delta^{15}N$ values of NH_4NO_3 samples. **b** Deviation of the nitrogen content (wt%) of the same NH_4NO_3 samples and standards from their known value. NH_4NO_3 samples and fertiliser display a difference of 2–3 %N from their expected value. **c** Zoom-in of the difference in the nitrogen content (%N) in the same sequence. Laboratory standards with an odd $\delta^{15}N$ value also displayed a slight offset in their difference in nitrogen content (% N) from the expected value

samples (memory effect). Finally, the repeatability and intensity of the phenomenon were not constant from one period of time to another.

Since there is a correlation between the type of material analysed just before the standard and its $\delta^{15}N$ value and nitrogen content, it appears that the IRMS system is not the cause of these odd measurements. We rather believe that this phenomenon is caused by nitrogen remaining in the EA system, either in the combustion reactor or in the reduction reactor, resulting from non-quantitative conversion of nitrate into N_2, which is then carried over to the next sample and released in subsequent analyses.

Peak shape A close examination of the chromatograms showed that the analysis of the laboratory standards produced a peak corresponding to well-eluted N_2. Even data displaying a disparate $\delta^{15}N$ value did not present any particularities. In contrast, the N_2 peak of KNO_3 and NH_4NO_3 exhibited tail (Fig. 4). At the same time, the *m*/*z* 29/28 ion current ratio was sluggish in its return to the baseline. The peak tailing indicates that either combustion or reduction (or both) is not occurring optimally and lingers. As peak tailing was observed for nitrates, but not for the organic laboratory standards, we assumed that this phenomenon specifically pertained to the conversion of nitrate into N_2.

Owing to tailing, all N_2 was not completely integrated as illustrated by the *m*/*z* 29/28 ratio in the upper part of Fig. 4. This explains the lower conversion of nitrates in terms of nitrogen content. Moreover, tailing led to variations in peak integration, which affected the repeatability of the $\delta^{15}N$ value.

Cleaning of the combustion tube or regeneration of copper in the reduction oven as well as replacement of the chemicals in both reactors neither eliminate the problem nor did it help to determine which reactor was the source of this behaviour. We performed a series of experiments in order to determine the cause of this phenomenon.

Part II: Investigations

Experiment 1: use of additives to improve combustion

The use of graphite and V_2O_5 as additives was investigated to assess if they could assist in the combustion. At first sight, the addition of graphite to nitrate-based samples improved the N_2 peak shape. Tailing was not observed any more and the precision of the $\delta^{15}N$ value was improved when graphite was added at 20 wt%. At higher mass of added graphite, the $\delta^{15}N$ value showed a larger variability. Yet, the $\delta^{15}N$ value of nitrate-containing compounds was clearly affected (Fig. 5, plot a). This was confirmed by the biased $\delta^{15}N$ value of

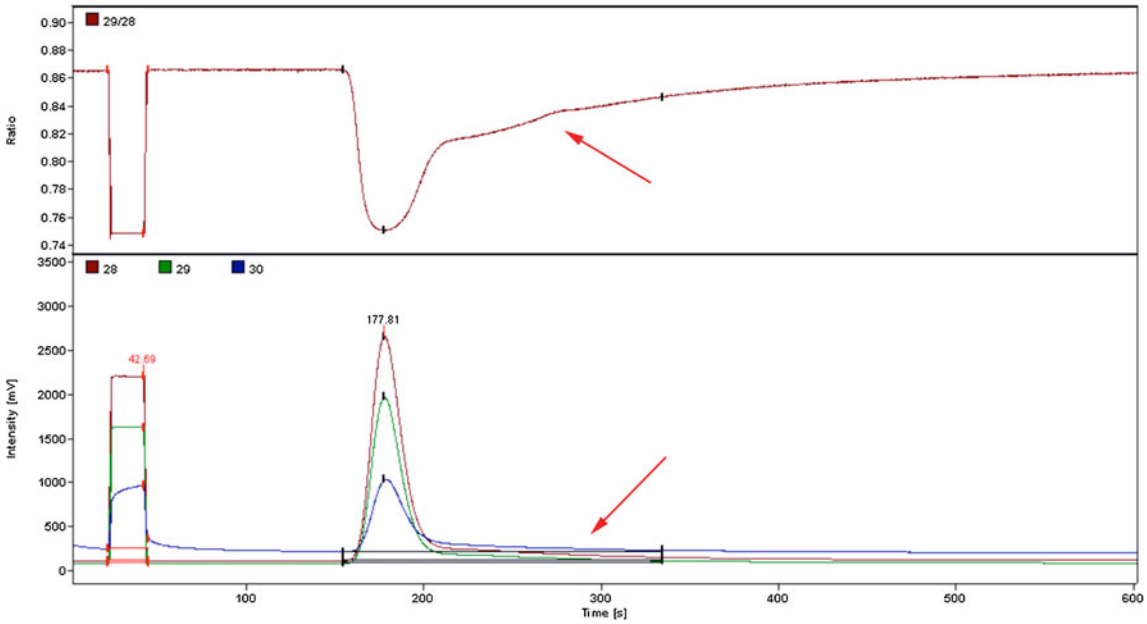

Fig. 4 δ^{15}N measurement of a KNO_3 sample. The N_2 peak of the sample exhbits tailing (*lower part*). This phenomenon is also visible from the *m/z* 29/28 ion current ratio (*upper part*), as highlighted by the *arrows*

IAEA-N1, IAEA-N2 and IAEA-NO-3 mixed with the additives (Fig. 5, plot b). The literature reveals that carbon residues resulting from incomplete combustion may retain nitrogen [18]. An alternative explanation is that incomplete combustion of carbon produces CO, which may be coeluted with N_2 and alter its accuracy because the molecules CO and N_2 have the same *m/z* (28 for $^{12}C^{16}O$ and $^{14}N^{14}N$ and 29 for $^{13}C^{16}O$ and $^{15}N^{14}N$). A closer look at the chromatograms revealed that the ion current ratio 29/28 did not completely return to the baseline before the CO. This incomplete return to the baseline of the ratio 29/28 is probably the reason for the difference between the measured and the expected δ^{15}N value.

The addition of V_2O_5 did not eliminate peak tailing and gave inaccurate results. In proportions greater than 20 wt% it led to tailing and affected peak resolution.

Experiment 2: use of an elemental analyser configuration with an additional copper section

Another elemental analyser configuration including an additional section of reduced copper (system 2) was used in order to see whether an incomplete reduction process was the cause of the observed tailing. Results were compared with those obtained with the usual elemental analyser configuration (system 1).

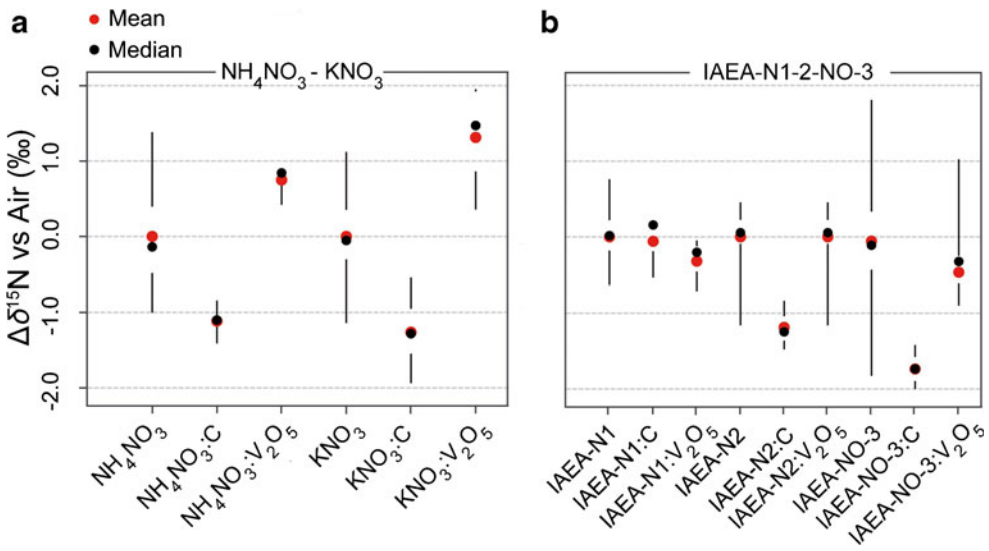

Fig. 5 The positions of the mean and median indicate the deviation the δ^{15}N value of the substance from its expected value. **a** Deviation of the δ^{15}N value of NH_4NO_3 and KNO_3 mixed with 20 wt% graphite and V_2O_5 from its original value (unmixed). **b** Deviation of the δ^{15}N values of international reference materials mixed with 20 wt% graphite and V_2O_5 from their known values

Peak shape The first replicates of IAEA-N1 and IAEA-N2 in the sequence showed a peak corresponding to well-eluted N_2 in systems 1 and 2. However, after a few replicates, the *m*/*z* 29/28 ratio of IAEA-N1 and IAEA-N2 either did not always perfectly return to the baseline or showed a baseline anomaly despite a peak corresponding to well-eluted N_2. These effects were observed in systems 1 and 2 (Figs. S1–S5).

Whereas the N_2 peak of IAEA-NO-3 exhibited tailing in system 1, N_2 appeared well eluted in system 2. The absence of tailing in system 2 was also observed for KNO_3 and NH_4NO_3 samples. In system 2, the upper layer of WO_3 is heated to 1,020 °C, whereas the lower electrolytic copper layer reaches a temperature of 850 °C. Nitrogen oxides are therefore reduced by two sections of metallic copper, one at 850 °C and another at 650 °C. These results support the hypothesis that tailing in system 1 is induced by incomplete reduction. This is also corroborated by the increased tailing when a compound rich in oxygen, such as V_2O_5, is added to a sample. However, as for IAEA-N1 and IAEA-N2, nitrates also exhibited a sluggish return to the baseline in terms of the *m*/*z* 29/28 ratio after the analysis of several replicates. In contrast, the organic laboratory standards showed a peak corresponding to well-eluted N_2 in both systems.

$\delta^{15}N$ values and nitrogen content The mean $\delta^{15}N$ values of IAEA-N1, IAEA-N2 and IAEA-NO-3 determined using both systems did not show any bias compared with the expected $\delta^{15}N$ value. Systems 1 and 2 produced a similar SD (0.3 ‰ for IAEA-N1 and IAEA-N2, 0.6 ‰ for IAEA-NO-3); however, it was larger than that reported in the literature (0.2 ‰ for IAEA-N1 and IAEA-N2 and 0.4 ‰ for IAEA-NO-3) [6]. Despite the absence of tailing in system 2, the repeatability of the $\delta^{15}N$ value was not improved.

Experiment 3: variations of the method parameters and exclusion of O_2

The modification of the O_2 pressure and helium flow did not improve the analytical results for nitrates. The sample delay (sample start and stop) was adapted in order to introduce the sample at different points in the analytical cycle (sample start at 0, 5, 10, 18, 55 and 62 s), whereas oxygen was injected for 60 s from the beginning of the analytical cycle. Finally, the exclusion of oxygen from the analytical cycle was also tested.

For IAEA-N1 and IAEA-N2, the best results were obtained without injection of O_2 or when the O_2 concentration was at its lowest level (sample introduced at 0 or 5 s) (Table 2, Fig. 6). Under these conditions, N_2 was well eluted and the *m*/*z* 29/28 ratio did not show any anomaly throughout repeated analyses. The intermediate repeatability of the $\delta^{15}N$ value for these compounds is excellent (0.1 ‰) and corresponds to the estimated expanded uncertainty (less than 0.1 ‰, k=2).

For IAEA-NO-3 and nitrate-containing samples, the exclusion of O_2 from the analytical cycle gave, on the contrary, a peak corresponding to well-eluted N_2 with an *m*/*z* 29/28 ratio returning perfectly to the baseline, even after ten replicates (Fig. 7), whereas all conditions involving O_2 injection did not produce satisfactory results. These analytical conditions produced excellent repeatability of the $\delta^{15}N$ value of 0.1 ‰, after exclusion of outliers when present. The estimated expanded uncertainty (k=2) associated with the $\delta^{15}N$ measurement of nitrates (IAEA-NO-3, KNO_3 and NH_4NO_3 samples) is 0.1 ‰.

Only the organic laboratory standards showed inconsistent results when analysed without oxygen, as expected. The incomplete combustion of organic material produces CO, which may interfere with N_2 if it is not eliminated by an adequate trap ($^{12}C^{16}O$ with m/z=28 and $^{13}C^{16}O$ with m/z=29). The best results were obtained using the usual settings of the analytical cycle (oxygen for 60 s, sample start/stop at 18 s/ 20s). These conditions favour the introduction of the organic sample in an oxygen-rich environment and ensure its complete combustion.

The $\delta^{15}N$ results are supported by the nitrogen content of the inorganic substances (Fig. 8). The values for the nitrogen content of IAEA-N1 and IAEA-N2 improved when the reference material was introduced at 0 or 5 s from the beginning of the analytical cycle (with O_2 injection). The results significantly improved when the substances were analysed without O_2, with a repeatability of 0.1–0.2 %. Whereas the analysis of nitrates (IAEA-NO-3, KNO_3 and NH_4NO_3) with O_2 always produced a lower nitrogen

Table 2 $\delta^{15}N$ values and standard deviation (*SD*) of international reference materials, analysed with system 1 with and without O_2 injection. All measurements (*N*) are included in the calculated means and standard deviations

International reference material	Mean $\delta^{15}N$ vs. air (‰) ± SD				
	With O_2	*N*	Without O_2	*N*	Known $\delta^{15}N$ values
IAEA-N1	0.4±0.3	67	0.4±0.1	46	0.4±0.2 [6]
IAEA-N2	20.3±0.3	53	20.3±0.1	50	20.3±0.2 [6]
IAEA-NO-3	4.5±0.6	71	4.7±0.2	50	4.7±0.4 [6]

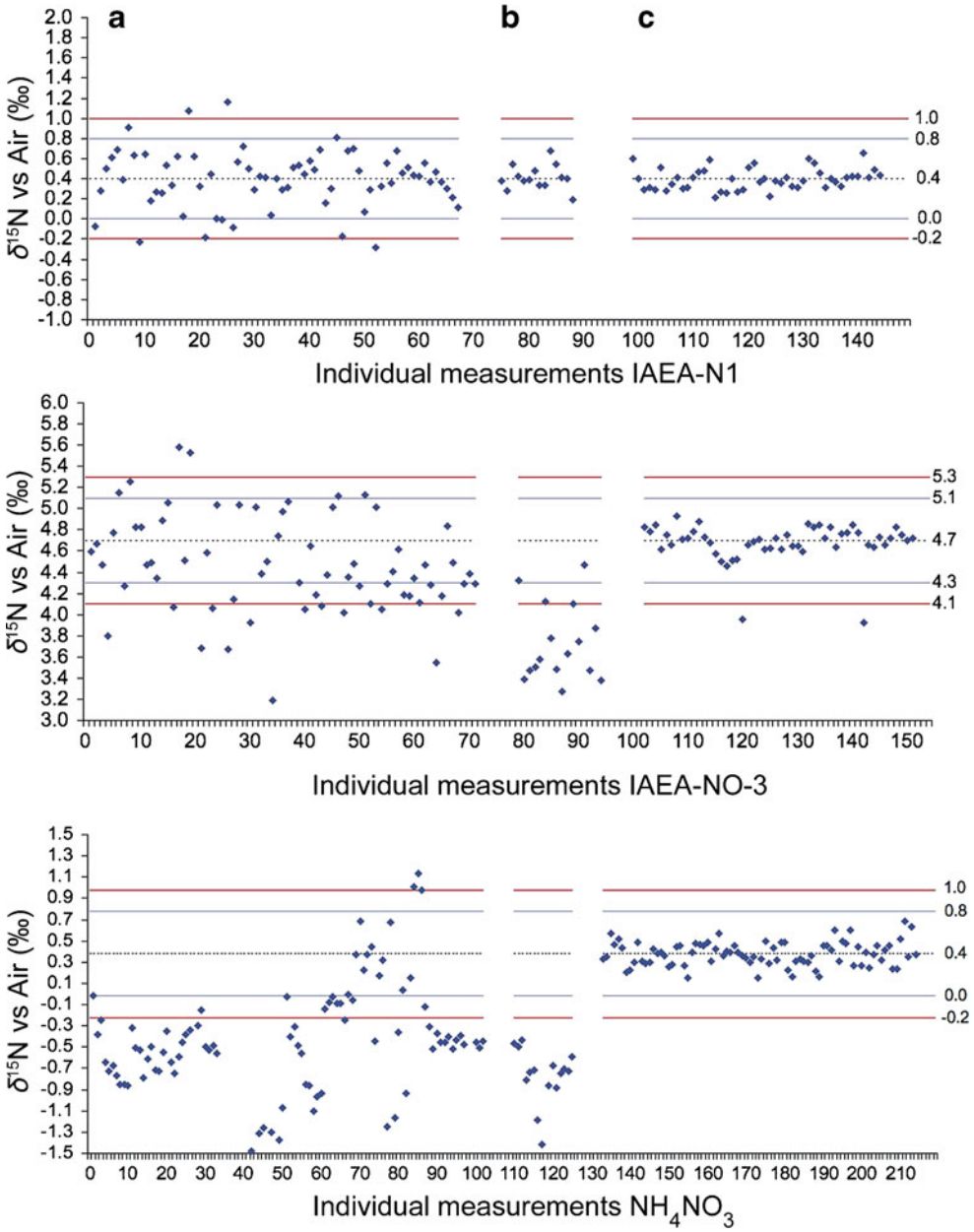

Fig. 6 Control charts of the δ^{15}N measurements of IAEA-N1 [$(NH_4)_2SO_4$], IAEA-NO-3 (KNO_3) and NH_4NO_3 samples analysed with system 1. **a** with oxygen injection (analytical cycle 70 s, oxygen for 60 s., sample start/stop at 18 s/20 s), **b** with oxygen injection (analytical cycle 70 s, oxygen for 60 s, sample start/stop at 0 s/2 s and 5 s/7 s), **c** without oxygen injection (analytical cycle 70 s, sample start/stop at 18 s/20 s). The expected δ^{15}N value is represented by a *central dotted black line*. For NH_4NO_3, the *dotted line* represents the mean value of measurements performed without oxygen. Upper and lower warning lines (*blue*) and action lines (*red*) are defined as two standard deviations and three standard deviations, respectively

content than expected, their analysis without O_2 yielded the expected nitrogen content with satisfactory repeatability (0.3–0.6 % for nitrates after exclusion of outliers).

Experiment 2 showed that the tailing of the N_2 peak of nitrates resulted from incomplete reduction. In 1973, Pella and Colombo [18] stated that the combustion of nitro compounds generated large quantities of nitrogen oxides which might not be quantitatively reduced. They also highlighted the influence of O_2 concentration on the determination of the nitrogen content of nitro compounds when performing EA. Nitro compounds dropped under maximum O_2 concentration resulted in inaccurate values for the nitrogen content. However, lower O_2 concentration favoured the reduction of nitrogen oxides and resulted in more accurate values for the nitrogen content.

The results of experiment 3 demonstrate the importance of the influence of oxygen on the δ^{15}N measurements of nitrate (KNO_3 and NH_4NO_3), but also of other inorganic compounds such as $(NH_4)_2SO_4$. In contrast to the study of Pella and Colombo, the introduction of nitrates at lower O_2 concentration (sample start at 0 or 5 s) did not produce satisfactory values for δ^{15}N and nitrogen content. Only the complete exclusion of oxygen from the analytical cycle led to excellent and repeatable results for nitrates.

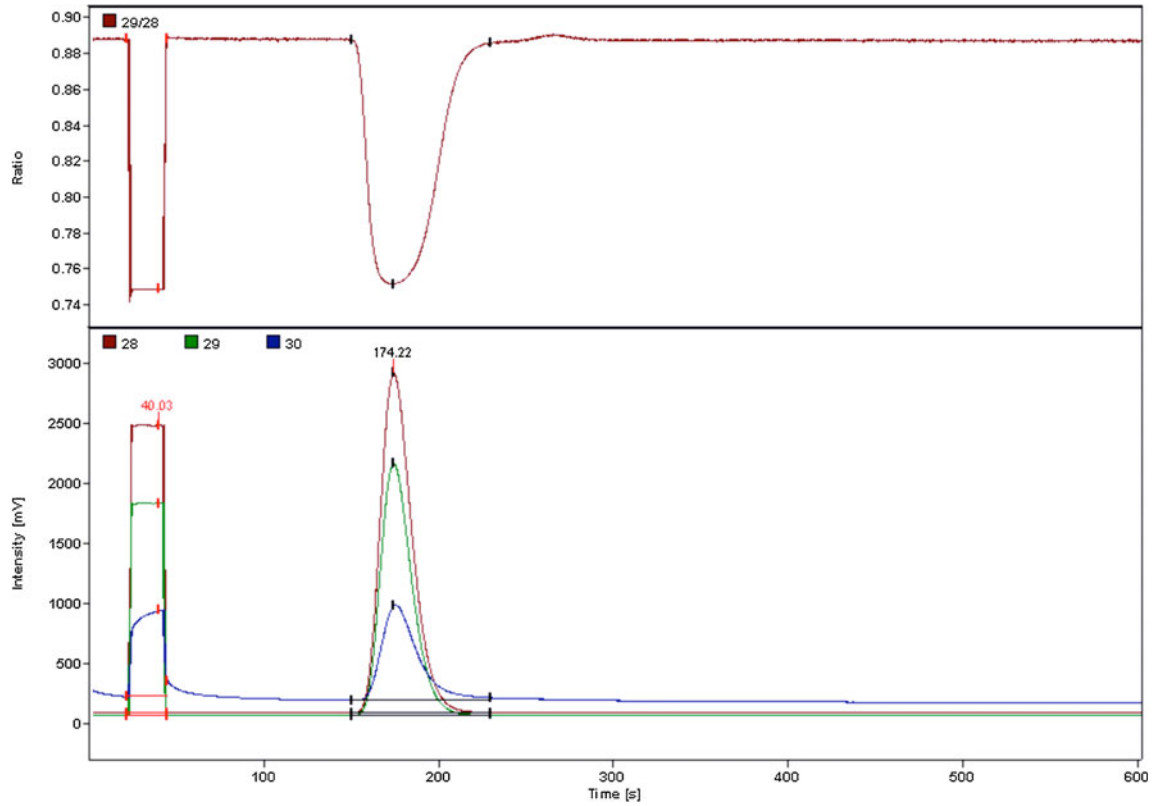

Fig. 7 $\delta^{15}N$ measurement of IAEA-NO-3 (KNO_3) obtained without oxygen injection (analytical cycle 70 s, sample start/stop at 18 s/20 s). The N_2 is well eluted and the peak does not show any tailing. In addition, the *m*/*z* 29/28 ion current ratio perfectly returns to the baseline even after ten replicates

The principle of the analytical technique is based on flash combustion, which is obtained through the sudden oxidation of tin in an oxygen-rich environment. This exothermic reaction produces a bright flash and instantly transforms the sample into gaseous combustion products at around 1,700 °C. Gaseous products are then carried through the reduction reactor for the oxides to be reduced. The requirement of injecting oxygen in excess to create an oxygen-rich environment is necessary for organic material, i.e. carbon-rich material, in order to ensure the complete oxidation of the sample. However, for highly oxidised inorganic substances such as nitrates where nitrogen assumes its highest possible oxidation number of+V, the injection of oxygen is not necessary when the sample is introduced and, even more so, is not advised. The following thermochemical considerations explain the reasons, taking into consideration the chemical nature of the substances as well as the physical and chemical conditions related to the method.

Thermochemical considerations

Using thermochemical methods [19, 20], the thermal decomposition and the equilibrium predictions of the compounds of interest explain our observations and provide guidance for performing proper laboratory procedures for reference materials. We will consider the processing of KNO_3, NH_4NO_3 and $(NH_4)_2SO_4$ as illustrative examples. Typically, a mass corresponding to roughly 2 mbar or approximately 2×10^{-3} atm of the nitrogen-containing compound is evaporated, filling a volume of approximately 50 cm^3. Runs with O_2 were performed at a partial pressure of 360 mbar, corresponding to 0.348 atm, in comparison with runs without added O_2. The present strategy consists of comparing the equilibria with and without added O_2 at temperatures of interest for each compound, considering the tables in the Appendix.

KNO_3 Crystalline KNO_3 is a stable salt whose high-temperature equilibrium is given by Eq. 1:

$$2KNO_3 \leftrightarrows K_2O + 2NO + 3/2O_2 \qquad (K_1) \qquad (1)$$

The forward direction of the equilibrium in Eq. 1 describes the high-temperature thermal decomposition starting at 1,070 K [21]. KNO_3 has been reported to decompose to potassium nitrite (KNO_2) according to Eq. 2. However, this decomposition path will not be considered in detail here because KNO_2 is less stable than the original material. In

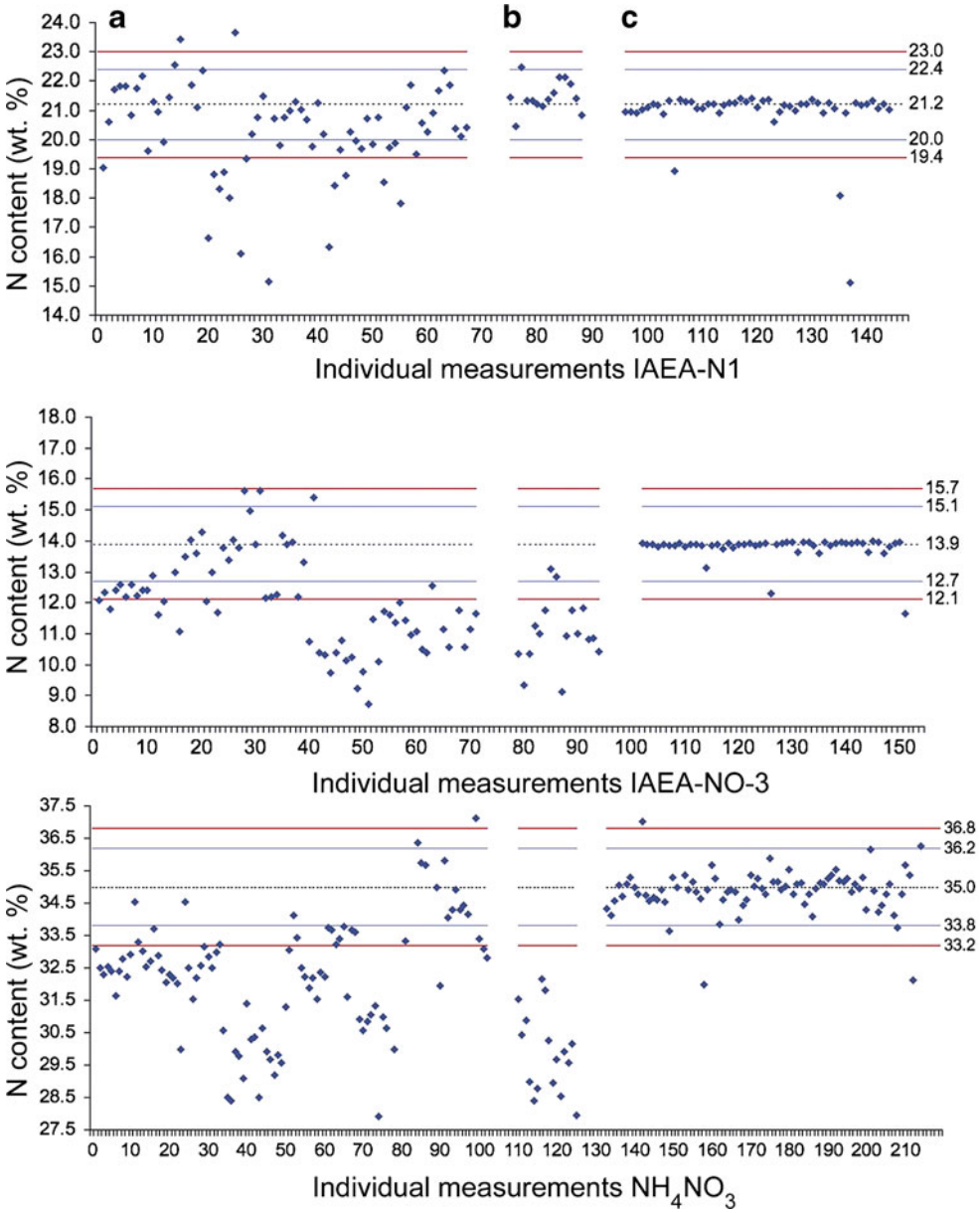

Fig. 8 Control charts of the nitrogen content of IAEA-N1 [$(NH_4)_2SO_4$], IAEA-NO-3 (KNO_3) and NH_4NO_3 samples obtained with system 1. **a** with oxygen injection (analytical cycle 70 s, oxygen for 60 s, sample start/stop at 18 s/20 s), **b** with oxygen injection (analytical cycle 70 s, oxygen for 60 s, sample start/stop at 0 s/2 s and 5 s/7 s), **c** without oxygen injection (analytical cycle 70 s, sample start/stop at 18 s/20 s). The expected nitrogen content is represented by a *central dotted black line*. Upper and lower warning lines (*blue*) and action lines (*red*) are defined as two standard deviations and three standard deviations, respectively

contrast to KNO_3, whose decomposition starts at 923 K when it is heated in air [21], the decomposition of KNO_2 starts at 700 K:

$$KNO_3 \leftrightarrows KNO_2 + 1/2O_2 \quad (2)$$

NO is the only oxide of nitrogen that is stable at temperatures in excess of 500–600 K because all other oxides of nitrogen, such as NO_2, N_2O_5, N_2O_4, N_2O_3 and N_2O_2, and oxyacids of nitrogen, such as HNO_3, HNO_4, HONO and $H_2N_2O_2$, convert to NO and O_2 at higher temperatures of interest. It therefore behoves us to consider the equilibrium in Eq. 1 as the relevant reaction sequence for the thermal decomposition of KNO_3. Of course, the equilibrium in Eq. 1 may be understood as the sum of the equilibria in Eqs. 3a and 3b, which underlines the thermal instability of N_2O_5:

$$2KNO_3 \leftrightarrows K_2O + N_2O_5 \quad (3a)$$

$$N_2O_5 \leftrightarrows 2NO + 3/2O_2 \quad (3b)$$

The relevant thermochemistry of the equilibrium in Eq. 1 is given in Table 3. Table 4 gives the ratio of the equilibrium

pressures of NO and O_2 in the absence of added O_2 (second column from the left) and in the presence of O_2 (third column) as a function of temperature. The ratio of NO or nitrogen in oxidation state+II to KNO_3 with nitrogen in oxidation state+V is given in columns 4 and 5 in the absence and presence of added O_2, respectively. Adding 360 mbar of O_2 to the carrier gas for thermal processing of KNO_3 shifts the equilibrium to the left, favouring nitrogen in its high oxidation state (+V) at the expense of NO [N(+II)]. This is just a consequence of Le Chatelier's principle, of which columns 4 and 5 are a clear manifestation. Finally, the last column of Table 4 displays the factor by which the equilibrium is shifted to the left by the presence of O_2. At temperatures exceeding 1,300 K, this factor ranges from 30 to 80. The corollary, therefore, is that the presence of O_2 shifts nitrogen closer to its oxidised form, whereas we require the inverse as we are ultimately interested in the reduction of NO to N_2 in the reducing part of the elemental analyser.

Of note is the position of the equilibrium in Eq. 4 with and without added O_2, the details being given in Table 5 (thermochemistry) and Table 6 (equilibrium pressures):

$$2NO_2 \leftrightarrows 2NO + O_2 \qquad (K_2) \qquad (4)$$

The equilibrium in Eq. 4 is important in combustion/exhaust systems and shows qualitatively the same behaviour as the equilibrium in Eq. 1 as a function of temperature: added O_2 shifts the equilibrium towards NO_2 [N(+IV)] at the expense of the less oxidised form of nitrogen, namely NO [N(+II)]. However, the equilibrium lies far to the right at temperatures exceeding 500 K without the addition of O_2. The third column of Table 6 shows a rapidly decreasing ratio $r=P_{NO2}/P_{NO}$ with and without the addition of O_2 for temperatures exceeding 500 K. The addition of a large amount of O_2 increases the relative NO_2 concentration by a factor of 18.68 at 1,000 K (fourth column of Table 6) over the values without addition of O_2 (third column of Table 6). The fifth column of Table 6 displays an r/r^{O2} ratio of roughly 20 at 1,000 K, which means that P_{NO2}/P_{NO} is 20 times larger in the presence of added O_2 than in its absence. The equilibria in Eqs. 1 and 4 are sufficiently decoupled as far as the temperature is concerned, and so one does not have to take into account the equilibrium in Eq. 4 when considering the decomposition of KNO_3 (Eq. 1). That is to say that the equilibrium in Eq. 4 will not change the speciation of nitrogen between NO and NO_2 at temperatures exceeding 1,000 K because the equilibrium in Eq. 1 specifies NO_x occurs in the form of NO, with or without the occurrence of the equilibrium in Eq. 4 owing to the high-temperature stability of NO compared with NO_2.

NH_4NO_3 NH_4NO_3 decomposes according to two principal channels displayed in Eqs. 5 and 6:

$$NH_4NO_3 \leftrightarrows NH_3 + HNO_3 \qquad (5)$$

$$NH_4NO_3 \leftrightarrows H_2O + NH_2NO_2 \leftrightarrows H_2O + N_2O \leftrightarrows N_2 + 1/2O_2 \qquad (6)$$

For the sake of simplicity, we will only consider the reaction in Eq. 5, which is faster than the nitramide branch (reaction in Eq. 6) under most experimental conditions. Tables 7 and 8 give the decomposition temperatures of NH_3 and HNO_3, respectively, these being two prototypical products often encountered in thermal processing. Table 7 reveals the inherent thermodynamic instability of NH_3 towards thermal decomposition, which is independent of added O_2:

$$2NH_3 \leftrightarrows N_2 + 3H_2 \qquad (K_3) \qquad (7)$$

However, the decomposition of HNO_3, which follows a mechanism proposed by Johnston et al. [22], is governed by the same principle as the decomposition of KNO_3 (Eq. 1) and NO_2 (Eq. 4) discussed above. HNO_3 is a fairly unstable species in the gas phase and releases O_2, which makes it sensitive to the presence of added O_2 according to the reaction in Eq. 8:

$$2HNO_3 \leftrightarrows H_2O + NO_2 + NO + O_2 \qquad (K_4) \qquad (8)$$

Table 9 reveals an r/r^{O2} ratio of approximately 20 in the 300–700 K temperature range: added O_2 shifts the equilibrium from NO and NO_2 towards HNO_3 i.e., back to the higher oxidation state, i.e. N(+II) and N(+IV) ➔ N(+V), as may be seen in Eq. 8. The fact that gas-phase HNO_3 decomposes at a relatively low temperature may perhaps come as a surprise.

$(NH_4)_2SO_4$ The pattern of thermal decomposition is similar to that for NH_4NO_3, namely

$$(NH_4)_2SO_4 \leftrightarrows 2NH_3 + H_2SO_4 \qquad (9)$$

$$H_2SO_4 \leftrightarrows SO_2 + H_2O + 1/2O_2 \qquad (K_5) \qquad (10)$$

H_2SO_4 is significantly stabler than HNO_3 as revealed in Table 10 (thermochemistry) and Table 11 (equilibrium pressures). H_2SO_4 is essentially quantitatively decomposed at 700 K and releases O_2, which makes it sensitive to added O_2 according to Eq. 10. In the present case, equilibrium constant K_5 shifts SO_2 [S(+IV)] to H_2SO_4 [S(+VI)] in agreement with $r/r^{O2}=10$ in the temperature range from 500 to 900 K (Table 11). However, the thermal stability of NH_3 (K_3) is independent of H_2SO_4 as far as the decomposition reaction (Eq. 7) in a non-oxidising atmosphere is concerned because NH_3 and H_2SO_4 do not have any decomposition products in common (reactions in Eqs. 7 and 10). Therefore, both decomposition products from the reaction in Eq. 9, namely NH_3 and H_2SO_4, behave independently of each other.

However, ammonia oxidation according to the reaction in Eq. 11 has to be considered in the case when O_2 is deliberately added to the carrier gas:

$$NH_3 + 5/4O_2 \leftrightarrows NO + 3/2H_2O \qquad (K_6) \qquad (11)$$

Equation 11 is valid for catalytic oxidation, which is of relevance in the present context, whereas direct (non-catalytic) air oxidation (combustion) leads to N_2 and H_2O vapour. Table 12 displays the thermochemical data for the range from 300 to 1,800 K, including the equilibrium constant K_6. Its values throughout the given temperature range are mainly given by the stability of product H_2O vapour, which controls the position of the equilibrium in Eq. 11 Any O_2 generated as a reaction product such as in the reaction in Eq. 10 will immediately undergo reaction with NH_3 to generate NO following Eq. 11. The primary reaction (Eq. 9) may be combined with the reactions in Eqs. 10 and 11 in the following way:

$$(NH_4)_2SO_4 + 5/2O_2 \leftrightarrows SO_2 + 2NO + 4H_2O + 1/2O_2 \qquad (12)$$

The decomposition of sulphuric acid (Eq. 10), only generates 0.5 mol O_2 of the 2.5 mol O_2 necessary for complete oxidation of NH_3 according to Eq. 11. This means that roughly 10 % or less of the evolving NH_3 from the reaction in Eq. 8 will be converted to NO according to Eq. 11 if equilibrium is established because roughly half of the oxygen is consumed to oxidise nitrogen to NO and the other half of the oxygen is used to oxidise the hydrogen of NH_3 to H_2O following Eq. 11. However, in the case of added oxygen, 100 % of ammonia will be catalytically oxidised to NO owing to the strong exothermicity of the reaction in Eq. 11, leading to the enormous values of K_6 in Table 12. NO, once generated, is difficult to reduce to N_2 [23], the species of interest in the present context. It is therefore concluded, as in the cases discussed above, that the addition of O_2 in reactions of thermal decomposition of species that are already in their highest oxidation state leads to an increased extent of oxidation of reaction products that will have to be reversed in the reduction stages of the elemental analyser (Fig. 1) in order to monitor nitrogen as N_2. It is possible that this re-reduction of oxidised forms of nitrogen will lead to losses or incomplete conversion in the present experimental protocol.

In conclusion, equilibria are shifted towards species with a higher oxidation state in the presence of added O_2 whenever the equilibrium decomposition involves the formation of O_2. This is a consequence of Le Chatelier's principle and may be quantitatively assessed using high-temperature thermochemistry. The shift towards species of higher oxidation states upon addition of O_2 amounts to factors of 10–80 of the equilibrium pressures depending on the specific thermochemistry. In the present case, one wants to preserve the low oxidation states in order to support quantitative conversion of oxidised nitrogen to N_2 for analytical purposes. Using a similar strategy, Révész et al. [24] used catalysed graphite combustion of nitrates at 800 K to trap O_2 as stable carbonates. In this way, O_2 was prevented from reoxidising nitrogen to a higher oxidation state.

Concluding remarks From a chemical point of view, "oxidation" of nitrates and sulphates, including HNO_3 and H_2SO_4, should be replaced by the term "thermal decomposition" because these compounds already exist in their highest possible oxidation state. Therefore, any further attempt at oxidation is chemically impossible and thus essentially counterproductive. Instead, decomposition changes the state of oxidation of nitrogen. Taking HNO_3 as an example (Eq. (8)), oxide ions [O (−II)] are oxidised to elementary O_2 by simultaneously reducing N(+V) to N(+IV) or N(+II) depending on the temperature. This internal change of oxidation state is thermodynamically driven by the stability of nitrogen oxides that increasingly favour the lower oxidation state of N(+II), i.e. NO in Eq. 8, over the higher oxidation states corresponding to NO_2 [N(+IV)] or HNO_3 [N(+V)] with increasing temperature. In addition, it is recognised that the reduction of NO to N_2 is difficult owing to kinetic control, especially at lower temperatures, a fact that may lead to losses of nitrogen and/or to unwanted side reactions not resulting in N_2, the product of interest. This view of high-temperature reactivity in itself, supported by the aforementioned thermochemical considerations, suggests the processing of oxidised nitrogen in the absence of added O_2. This shows that it is inadequate to analyse inorganic and organic substances in the same sequence using the same method, as they

undergo different thermal decomposition or combustion reactions.

The addition of sucrose and/or other oxidisable material (graphite) in nitrate decomposition experiments serves to remove (i.e. oxidise) the product O_2 but does not affect the decomposition reaction itself [1, 7–9].

Implications for the calibration of organic laboratory standards with inorganic International Atomic Energy Agency reference materials

Secondary international reference materials IAEA-N1, IAEA-N2 and IAEA-NO-3 are used to calibrate the IRMS system and the organic laboratory standards. A common procedure to calibrate a material (the future laboratory standard) is to analyse replicates of the substance with the international reference materials IAEA-N1, IAEA-N2 and IAEA-NO-3 in the same analytical sequence. This procedure, however, requires the same analytical procedure to be used for the material and the secondary international reference material. As demonstrated by our results, organic material and inorganic substances, such as $(NH_4)_2SO_4$ (IAEA-N1 and IAEA-N2) and KNO_3 (IAEA-NO-3), should not be analysed using the same analytical procedure because of their different chemical nature. The limited accessibility of organic international reference materials constrains the isotope community to use the inorganic IAEA-N1, IAEA-N2 and IAEA-NO-3 for the calibration of organic laboratory standards to the international scale.

Thus, on the basis of our results, when an organic material has to be calibrated against IAEA-N1, IAEA-N2 and IAEA-NO-3, we suggest calibrating the IRMS system by analysing IAEA-N1, IAEA-N2 and IAEA-NO-3 without oxygen first. Then, the $\delta^{15}N$ value of the future organic standard may be obtained by analysing replicates of organic material in the presence of oxygen with the calibrated IRMS system, and ideally using an organic certified reference material.

Conclusion

An unexpected series of $\delta^{15}N$ values in our laboratory standards were observed when analysing nitrates and organic laboratory standards in the same analytical sequence. A closer examination of the chromatograms showed that the N_2 peaks of nitrates exhibited tails, thus affecting the repeatability of the $\delta^{15}N$ values of nitrate and laboratory standards. A series of experiments were conducted to understand the cause of this phenomenon. In experiment 1, the use of additives to sustain combustion did not produce conclusive results. The addition of graphite to samples produced biased $\delta^{15}N$ values, whereas the addition of V_2O_5 increased the tailing of the N_2 peaks. In experiment 2, additional tests were undertaken with another elemental analyser configuration (system 2) involving a supplementary copper section. The results revealed that the tailing of nitrates originated from an incomplete reduction process. Nevertheless, despite the absence of tailing in system 2, the repeatability of the $\delta^{15}N$ values was not improved much.

Finally, modifications of the method parameters were undertaken in experiment 3. For IAEA-N1 and IAEA-N2, the introduction of the sample at 0 or 5 s after the beginning of the analytical cycle (with O_2 injection), or when oxygen was excluded, provided excellent repeatability of $\delta^{15}N$ values (0.1 ‰) without outliers. Although the exclusion of oxygen from the analytical procedure was not adequate for organic standards, the analytical procedure performed excellently and produced repeatable $\delta^{15}N$ values with only rare outliers for KNO_3 and NH_4NO_3. Under these conditions, the estimated expanded uncertainty (k=2) associated with the $\delta^{15}N$ measurement of nitrates and of ammonium sulphate compounds is 0.1 ‰. These settings also allowed a much better recovery of nitrogen, especially for KNO_3, than the analysis with O_2 injection.

We showed that organic compounds, on the one hand, and nitrates and ammonium sulphate (IAEA-N1 and IAEA-N2), on the other hand, should not be analysed using the same analytical procedure, given their different chemical nature. Although the instrumental technique was developed to transform the sample into simple gases by means of flash combustion, the thermodynamic considerations demonstrate that not all materials behave in the same way because of their different chemical nature. This aspect needs to be taken into consideration when using EA-IRMS and upholds the principle to use laboratory standards with a chemical structure as similar as possible to that of the samples. This necessarily impacts on the way inorganic secondary reference materials should be used for the calibration of organic laboratory standards.

Acknowledgments The authors thank Catharina Lötscher and Matthias Saurer for their help with the numerous isotopic analyses. They also acknowledge Thomas Kuhn and Oliver Kracht from Thermo Fisher Scientific for their valuable reflections and advice on this issue. The authors are also grateful to the anonymous reviewers for their helpful comments and suggestions regarding the manuscript. This research was partly funded by the Fondation du 450ème Anniversaire de l'Université de Lausanne and the Société Académique Vaudoise.

Appendix

Tables 3, 4, 5, 6, 7, 8, 9, 10, 11, and 12 provide supplementary material for thermochemical evaluation of standard reactions (standard state: 1 atm).

Table 3 Thermochemical data for the equilibrium in Eq. 1

T/K	ΔH^0_r/kcal/mol	ΔS^0_r/cal/molK	ΔG^0_r/kcal/mol	K_1/(atm)$^{5/2}$
300	176.33	93.87	148.17	1.00 (−108)
800	175.80	93.53	100.97	2.51 (−28)
1,000	174.85	92.48	82.36	9.74 (−19)
1,100	174.32	91.93	73.19	2.82 (−15)
1,200	173.50	91.30	63.95	2.22 (−12)
1,300	172.46	90.46	54.87	5.90 (−10)
1,400	170.83	89.25	45.88	6.82 (−8)
1,500	168.27	87.46	37.08	3.93 (−6)
1,600	160.39	84.91	24.53	4.43 (−4)
1,700	158.46	81.32	20.21	2.51 (−3)
1,800	149.70	76.40	12.18	3.31 (−2)

Thermochemical data for KNO_3 and K_2O for the hypothetical gas phase were taken from [20]; data for NO and O_2 were taken from [19]. The thermochemistry as a function of temperature for KNO_3 and K_2O was evaluated using the seven-coefficient NASA polynomial fitting for the range from 300 to 1,000 K given in [20]. A number within *parentheses* is the exponent (base 10). For example, 2.45 (−5) is 2.45×10^{-5}.

Table 5 Thermodynamic data for the equilibrium in Eq. 4

T/K	ΔH^0_r/kcal/mol	ΔS^0_r/cal/molK	ΔG^0_r/kcal/mol	K_2/atm
300	27.34	35.03	16.83	5.46 (−13)
400	27.64	35.87	13.26	5.67 (−8)
500	27.82	36.28	9.68	5.87 (−5)
1,000	27.94	36.51	−8.57	74.67
1,100	27.90	36.49	−12.24	270.31
1,200	27.84	36.45	−15.90	7.87.1
1,300	27.80	36.40	−19.52	1.913 (3)
1,400	27.74	36.36	−23.16	4.13 (3)
1,800	27.52	36.23	−37.69	3.77 (4)

Thermochemical information for NO_2, NO and O_2 was taken from [19]. A number within *parentheses* is the exponent (base 10). For example, 2.45 (−5) is 2.45×10^{-5}.

Table 4 Equilibrium pressures of NO and O_2 for the equilibrium in Eq. 1 at an initial pressure of KNO_3 of 2.0×10^{-3} atm (r) and at a prescribed O_2 partial pressure of 0.348 atm (r^{O2})

T/K	x	x (for O_2 partial pressure of 0.348 atm)	$2x/(2\times10^{-3} - 2x)$ (r)	$2x/(2\times10^{-3} - 2x)$ (r^{O2})	r/r^{O2}
800	3.7575 (−8)	1.2348 (−11)	3.76 (−5)	1.24 (−8)	3,042.9
1,000	5.0675 (−6)	1.9405 (−8)	5.09 (−3)	1.94 (−5)	262.5
1,100	2.9462 (−5)	2.7652 (−7)	3.04 (−2)	2.77 (−4)	109.8
1,200	1.2390 (−4)	2.5494 (−6)	1.41 (−1)	2.56 (−3)	55.3
1,300	3.7000 (−4)	1.6240 (−5)	5.87 (−1)	1.65 (−2)	35.6
1,400	7.2983 (−4)	7.5882 (−5)	2.701	8.21 (−2)	32.9
1,500	9.3748 (−4)	2.5409 (−4)	14.99	3.41 (−1)	44.02
1,600	9.93293 (−4)	6.8738 (−4)	148.10	2.199	67.35
1,700	9.97158 (−4)	8.2676 (−4)	350.86	4.772	73.52
1,800	9.99214 (−4)	9.4198 (−4)	1271.3	16.236	78.30

$P_{NO} = 2x$, $P_{O2} = 0.75P_{NO}$. x satisfies the governing equation $(3/4)^{3/2}x^{9/2} - K_1(10^{-3} - x)^2 = 0$ for 2.0×10^{-3} atm and $x^3[(3/4)0.348]^{3/2} - K_1(10^{-3} - x)^2 = 0$ for the prescribed O_2 partial pressure. A number within *parentheses* is the exponent (base 10). For example, 2.45 (−5) is 2.45×10^{-5}.

Table 6 Equilibrium pressures of O_2 for the equilibrium in Eq. 4 at an initial pressure of NO_x of 2.0×10^{-3} atm (r) and at a prescribed O_2 partial pressure of 0.348 atm (r^{O2})

T/K	P_{O2}/atm	$P_{NO2}/P_{NO} = r$	$(P_{NO2}/P_{NO})^{O2}$	r^{O2}/r
300	1.63 (−6)	1,226	8.00 (5)	657.5
400	7.49 (−5)	25.7	2.48 (3)	96.4
500	6.10 (−4)	4.38 (−1)	67.99	175.8
1,000	1.99274 (−3)	3.64 (−3)	6.80 (−2)	18.68
1,100	1.99616 (−3)	1.92 (−3)	3.60 (−2)	18.75
1,200	1.99775 (−3)	1.13 (−3)	2.10 (−2)	18.58
1,300	1.99855 (−3)	7.25 (−4)	1.40 (−2)	19.31
1,400	1.99901 (−3)	4.95 (−4)	9.20 (−3)	18.58
1,800	1.99968 (−3)	1.60 (−4)	3.00 (−3)	18.75

$P_{NO} = x$. x satisfies the governing equation $0.5x^3 - K_2(2.0\times10^{-3} - x)^2 = 0$ for 2.0×10^{-3} atm NO_x and $P_{NO2}/P_{NO} = (y/K_2)^{1/2}$, with y being the prescribed O_2 partial pressure of 0.348 atm. A number within *parentheses* is the exponent (base 10). For example, 2.45 (−5) is 2.45×10^{-5}.

Table 8 Thermodynamic data for decomposition of HNO_3 (Eq. 8)

T/K	ΔH^0_r/kcal/mol	ΔS^0_r/cal/molK	ΔG^0_r/kcal/mol	K_4/(atm)^2
300	35.91	74.38	13.60	1.23 (−10)
400	36.26	75.32	6.13	4.44 (−4)
500	36.31	75.37	−1.38	4.00 (0)
600	36.22	75.04	−8.80	1.62 (3)
700	35.97	74.55	−16.22	1.16 (5)
800	35.63	74.00	−23.57	2.77 (6)
900	35.24	73.46	−30.87	3.17 (7)
1,000	34.82	72.94	−38.12	2.17 (8)
1,100	34.36	72.42	−45.30	1.01 (9)
1,200	33.88	71.89	−52.39	3.52 (9)
1,300	33.39	71.28	−59.27	9.35 (9)
1,400	32.88	70.54	−65.88	1.95 (10)

Thermochemical data for HNO_3 were obtained from [20]; data for H_2O, O_2, NO_2 and NO were taken from [19]. The thermochemistry as a function of temperature for HNO_3 was evaluated using the seven-coefficient NASA polynomial fitting for the range from 300 to 1,000 K given in [20]. A number within parentheses is the exponent (base 10). For example, 2.45 (−5) is 2.45×10^{-5}.

Table 7 Thermodynamic data for decomposition of NH_3 (Eq. 7) and partial pressure of N_2 with an initial pressure of NH_3 of 2.0×10^{-3} atm

T/K	ΔH^0_r/kcal/mol	ΔS^0_r/cal/molK	ΔG^0_r/kcal/mol	K_3/(atm)^2	P_{N2}(atm)	P_{N2}/P_{NH3}
300	21.96	47.39	7.74	2.28 (−6)	5.25 (−4)	0.553
400	22.96	46.63	4.30	4.43 (−3)	9.63745 (−4)	13.3
500	23.84	52.26	−2.29	10.02	9,99741 (−4)	1,930
600	24.56	53.56	−7.57	5.75 (2)	9.99892 (−4)	4.63 (3)
700	25.16	54.49	−12.98	1.13 (4)	9.99976 (−4)	2.08 (4)
800	25.64	55.15	−18.48	1.12 (5)	9.99992 (−4)	6.25 (4)
900	26.04	55.62	−24.02	6.81 (5)	9.99997 (−4)	1.66 (5)
1,100	26.54	56.11	−35.18	9.78 (6)	9.99999 (−4)	>5.0 (5)
1,300	26.78	56.31	−46.42	6.38 (7)	1.0 (−3)	–
1,800	40.08	56.21	−61.10	2.62 (7)	1.0 (−3)	–

$P_{N2} = 1/3P_{H2} = x$. x satisfies the governing equation $27x^4 - K_3(2.0\times10^{-3} - 2x)^2 = 0$. All thermochemical data were taken from [19]. A number within *parentheses* is the exponent (base 10). For example 2.45 (−5) is 2.45×10^{-5}.

Table 9 Partial pressure of O_2 at equilibrium (Eq. 8) for an initial pressure of HNO_3 of 2.0×10^{-3} atm and a prescribed O_2 pressure of 0.348 atm

T/K	$P_{H2O} = P_{O2}$	$P_{O2}/P_{HNO3} = r$	$P_{NO} = P_{NO2}$	$P_{O2}/P_{HNO3} = r^{O2}$	r/r^{O2}
300	1.38255 (−4)	8.02 (−2)	1.114 (−5)	5.633 (−3)	14.24
400	9.77335 (−4)	2.15 (1)	7.26112 (−4)	1.326	16.21
500	9.9975 (−4)	1.999 (3)	9.95369 (−4)	1.0747 (2)	18.60
600	9.99988 (−4)	4.166(4)	9.99768 (−4)	2.155 (3)	19.33
700	9.99999 (−4)	5.00 (5)	9.99973 (−4)	1.852 (4)	26.99
800	1.00 (−3)	–	9.99994 (−4)	8.333 (4)	
900	1.00 (−3)	–	9.99998 (−4)	2.500 (5)	
1,000	1.00 (−3)	–			

$P_{H2O} = P_{NO} = P_{NO2} = P_{O2} = x$. x satisfies the governing equation $x^4 - 4K_4(10^{-3} - x)^2 = 0$ for an initial pressure of HNO_3 of 2.0×10^{-3} atm and $0.348x^3 - 4K_4(10^{-3} - x)^2 = 0$ for a prescribed O_2 pressure of 0.348 atm. A number within *parentheses* is the exponent (base 10). For example, 2.45 (−5) is 2.45×10^{-5}.

[a] Extrapolated value based on assumed (average) value $r/r^{O2} = 20.0$ and r^{O2} at 600 K.

Table 10 Thermodynamic data for decomposition of H_2SO_4 (Eq. 10)

T/K	ΔH^0_r/kcal/mol	ΔS^0_r/cal/mol K	ΔG^0_r/kcal/mol	K_5/(atm)$^{3/2}$
300	48.26	59.80	30.32	7.90 (−23)
500	48.15	59.58	18.36	9.33 (−9)
700	47.52	58.55	6.54	9.09 (−3)
800	47.12	58.01	0.71	0.639
900	46.70	57.51	−5.06	16.95
1,000	46.24	57.04	−10.80	230.06
1,100	45.78	56.60	−16.48	1889.6
1,200	45.30	56.19	−22.13	1.08 (4)

All thermochemical data were taken from [19]. A number within *parentheses* is the exponent (base 10). For example, 2.45 (−5) is 2.45×10^{-5}.

Table 11 Partial pressure of O_2 at equilibrium (Eq. 10) for an initial H_2SO_4 pressure of 2.0×10^{-3} atm and a prescribed O_2 pressure of 0.348 atm

T/K	P_{SO2}	$P_{SO2}/P_{H2SO4} = r$	P_{SO2}	$P_{SO2}/P_{H2SO4} = r^{O2}$	r/r^{O2}
300	1.37933 (−10)	6.897 (−8)	6.73812 (−13)	3.369 (−10)	204.7
500	5.8004 (−5)	2.990 (−2)	7.30922 (−6)	3.668 (−3)	8.15
700	1.98632 (−3)	145.2	1.86661 (−3)	13.994	10.38
800	1.99980 (−3)	9.999 (3)	1.99783 (−3)	9.206 (2)	10.86
900	1.99999 (−3)	1.999 (5)	1.99992 (−3)	2.499 (4)	7.99
1,000	2.0 (−3)	–	1.99999 (−3)	1.999 (5)	–
1,100	2.0 (−3)	–	2.0 (−3)	–	–

$P_{SO2} = P_{H2O} = 2P_{O2} = x$. x satisfies the governing equation $x^{5/2} - (2)^{1/2}K_5(2.0\times10^{-3} - x) = 0$ for an initial pressure of H_2SO_4 of 2.0×10^{-3} atm and $0.348x^2 - K_5(2.0\times10^{-3} - x) = 0$ for a prescribed O_2 pressure of 0.348 atm. A number within *parentheses* is the exponent (base 10). For example, 2.45 (−5) is 2.45×10^{-5}.

Table 12 Thermodynamic data for catalytic oxidation of NH_3 (Eq. 11)

T/K	ΔH^0_r/kcal/mol	ΔS^0_r/cal/mol K	ΔG^0_r/kcal/mol	K_6/(atm)$^{1/4}$
300	−54.14	10.74	−57.36	6.50 (41)
500	−53.91	11.37	−59.60	1.16 (26)
700	−53.89	11.41	−61.89	2.14 (19)
800	−53,95	11.35	−63.03	1.69 (17)
900	−53.99	11.28	−64.14	3.85 (15)
1,000	−54.09	11.18	−65.27	1.88 (14)
1100	−54.19	11.09	−66.27	1.58 (13)
1,200	−54.32	10.98	−67.50	2.00 (12)
1,300	−54.43	10.87	−68.56	3.41 (11)
1,800	−55.13	10.43	−73.90	9.51 (8)

All thermochemical data were taken from [19]. A number within *parentheses* is the exponent (base 10). For example, 2.45 (−5) is 2.45×10^{-5}.

References

1. Aranda R IV, Stern LA, Dietz ME, McCormick MC, Barrow JA, Mothershead RF II (2011) Forensic utility of isotope ratio analysis of the explosive urea nitrate and its precursors. Forensic Sci Int 206 (1–3):143–149. doi:10.1016/j.forsciint.2010.07.030
2. Benson SJ, Lennard CJ, Hill DM, Maynard P, Roux C (2010) Forensic analysis of explosives using isotope ratio mass spectrometry (IRMS)—part 1: instrument validation of the DELTA XP IRMS for bulk nitrogen isotope ratio measurements. J Forensic Sci 55(1):193–204. doi:10.1111/j.1556-4029.2009.01241.x
3. Benson S (2009) Introduction of isotope ratio mass spectrometry (IRMS) for the forensic analysis of explosives. University of Technology of Sydney, Sydney
4. Benson SJ, Lennard CJ, Maynard P, Hill DM, Andrew AS, Neal K, Stuart-Williams H, Hope J, Stewart Walker G, Roux C (2010) Forensic analysis of explosives using isotope ratio mass spectrometry (IRMS)—part 2: forensic inter-laboratory trial: bulk carbon and nitrogen stable isotopes in a range of chemical compounds (Australia and New Zealand). J Forensic Sci 55(1):205–212. doi:10.1111/j.1556-4029.2009.01242.x
5. Forensic Isotope Ratio Mass Spectrometry Network (2011) FIRMS newsletter Spring 2011. Forensic Isotope Ratio Mass Spectrometry. Network, Bristol
6. Böhlke JK, Coplen TB (1993) Interlaboratory comparison of reference materials for nitrogen isotope ratio measurements. In: 5th IAEA meeting on stable isotope standards and intercomparison materials, Vienna. IAEA-TECDOC-825. International Atomic Energy Agency, Vienna, pp 51–62
7. Silva SR, Kendall C, Wilkinson DH, Ziegler AC, Chang CCY, Avanzino RJ (2000) A new method for collection of nitrate from fresh water and the analysis of nitrogen and oxygen isotope ratios. J Hydrol 228:22–36
8. Spoelstra J, Schiff SL, Jeffries DS, Semkin RG (2004) Effect of storage on the isotopic composition of nitrate in bulk precipitation. Environ Sci Technol 38(18):4723–4727
9. Noguchi J (1951) Improved method for quantitative nitrogen analysis of organic compounds. Sci Pap Osaka Univ 22(1):1–14
10. Borda P, Hayward LD (1967) Nitrogen analysis of nitrate esters by micro-Dumas combustion. Anal Chem 39(4):548–549
11. Schindler FV, Knighton RE (1999) Sample preparation for total nitrogen and 15N ratio analysis by the automated Dumas combustion method. Commun Soil Sci Plant 30(9–10):1315–1324
12. ISOGEOCHEM (2012) An e-mail discussion list and reference web site for stable isotope geochemistry. http://isogeochem.wikispaces.com/
13. Coplen TB (2011) Guidelines and recommended terms for expression of stable-isotope-ratio and gas-ratio measurement results. Rapid Commun Mass Spectrom 25:2538–2560
14. Paul D, Skrzypek G, Forizs I (2007) Normalization of measured stable isotopic compositions to isotope reference scales—a review. Rapid Commun Mass Spectrom 21(18):3006–3014. doi:10.1002/rcm.3185
15. Taverniers I, De Loose M, Van Bockstaele E (2004) Trends in quality in the analytical laboratory. II. Analytical method validation and quality assurance. Trends Anal Chem 23(8):535–552
16. Miller JN, Miller JC (2005) Statistics and chemometrics for analytical chemistry. Pearson, Harlow
17. Joint Committee for Guides in Metrology (2008) Evaluation of measurement data—guide to the expression of uncertainty in measurement. JCGM 100:2008. Bureau International des Poids et des Mesures, Paris
18. Pella E, Colombo B (1973) Study of carbon, hydrogen and nitrogen determination by combustion-gas chromatography. Mikrochim Acta 5:697–719
19. Stull DR, Prophet H (1971) JANAF thermodynamical tables, 2nd edn. US National Bureau of Standards. Office of Standards Reference Materials, Washington
20. Burcat A, Ruscic B (2005) Third millennium ideal gas and condensed phase thermochemical database for combustion with updates from active thermochemical tables, vol ANL-05/20. Argonne technical publication. See also http://garfield.chem.elte.hu/Burcat/burcat.html
21. Stern KH (2001) High temperature properties and thermal decomposition of inorganic salts with oxyanions. CRC, Boca Raton
22. Johnston HS, Foering L, Thompson RJ (1953) Kinetics of the thermal decomposition of nitric acid vapor. II. Mechanism. J Phys Chem 57(4):390–395
23. Degobert P (1992) Automobile et pollution. Technip, Paris
24. Révész K, Böhlke JK, Yoshinari T (1997) Determination of $\delta^{18}O$ and $\delta^{15}N$ in nitrate. Anal Chem 69(21):4375–4380